THE JOURNAL OF PHYSICAL CHEMISTRY Letters

Letter

pubs.acs.org/JPCL

Prospect of Retrieving Vibrational Wave Function by Single-Object Scattering Sampling

Hosung Ki,[†,‡,⊥] Kyung Hwan Kim,[†,‡,⊥] Jeongho Kim,[§] Jae Hyuk Lee,[†] Joonghan Kim,[∥] and Hyotcherl Ihee*[,†,‡]

[†]Department of Chemistry, KAIST, Daejeon 305-701, Republic of Korea

[‡]Center for Nanomaterials and Chemical Reactions, Institute for Basic Science (IBS), Daejeon 305-701, Republic of Korea

[§]Department of Chemistry, Inha University, Incheon 402-751, Republic of Korea

[∥]Department of Chemistry, The Catholic University of Korea, Bucheon 420-743, Republic of Korea

Supporting Information

ABSTRACT: The exact shape of wave functions has never been directly measured because an ensemble measurement is often overwhelmed by the contributions of highly populated configurations. In this work, we explore the possibility of directly obtaining vibrational wave functions by single-object scattering sampling (SOSS) using intense, ultrashort X-ray pulses provided by X-ray free electron lasers. Previously, single-molecule diffraction experiments using femtosecond X-ray pulses have been proposed with the prospect of determining three-dimensional structure of macromolecules without the need of single-crystal samples. In contrast to the previous proposals, SOSS is designed for obtaining the structural variations of constantly fluctuating molecules by sampling many single-shot, single-object scattering patterns. From the simulations on iodine molecules adopting various pulse characteristics and molecular parameters, we were able to reconstruct vibrational wave functions of molecular iodine and found that SOSS is feasible under appropriate experimental conditions.

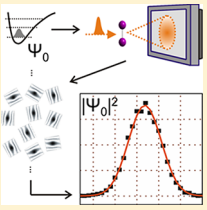

SECTION: Molecular Structure, Quantum Chemistry, and General Theory

A molecule continuously fluctuates by changing its molecular structure. Such fluctuations include vibration, rotation, bond dissociation, and bond formation, which are important for understanding chemical and physical properties of an object. Nevertheless, the exact shape of the structural phase space spanned by such structural fluctuations is highly elusive and has not been experimentally measured even for a simple molecule. This difficulty arises because a typical signal measured for a bulk sample contains contributions from all available structures mixed together. Single-molecule measurements may not suffer this ensemble average problem, but most common single-molecule techniques cannot capture the fluctuation of molecular structure due to the lack of either spatial or time resolution.[1−5] To overcome these problems that obstruct the direct probing of structural fluctuations, we here examine the feasibility of a novel single-molecule experimental scheme, which was proposed earlier by our group.[6] Our strategy is quite straightforward. First, we choose to use X-ray or electron diffraction as a probe because direct structural information needs to be extracted from single-molecule measurement. Second, the probe should be in the form of a sufficiently short pulse so that an instant of fast structural fluctuation can be captured as if the molecule is frozen in time. Third, each probe pulse should be intense enough so that the single-molecule diffraction induced by a single shot of the probe pulse can be detectably strong; otherwise, the time resolution will deteriorate by the averaging of many shots of measurements over time. Each of the resultant single-shot, single-molecule diffraction signals would contain the structural information of the molecule at the instant of the interaction between the probe pulse and the molecule. Collection of a sufficient number of such single-shot, single-molecule diffraction patterns will unveil the structural variations induced by fluctuations. In total, we need a sufficiently short and intense pulse of X-rays or electrons to realize this idea. Recent development of X-ray free-electron lasers (XFELs) has promised that such a scheme may be feasible in the future.

In our recent proposal of this novel experimental scheme, called single-object scattering sampling (SOSS),[6] the instantaneous structure of a single object is extracted from a single-shot, single-object scattering image obtained using an intense and extremely short X-ray pulse. By repeatedly capturing the snapshots of the object, we can sample a phase space representing all the possible structures involved in the structural fluctuation. We use the term "object" instead of "molecule" because this technique can be potentially applied to any objects such as small molecules, proteins, nucleic acids, macromolecular complexes, and nanoscale systems. At a glance, SOSS may appear similar to the single-molecule diffraction methods proposed earlier for structural characterization of biological molecules since both methods make use of single-shot, single-molecule diffraction images to obtain structural information of the target molecule. However, we note that the ways of data processing and thus the information contents

Received: August 1, 2013
Accepted: September 19, 2013

   dx.doi.org/10.1021/jz4016298 | J. Phys. Chem. Lett. 2013, 4, 3345−3350

obtained by the two techniques are different from each other. In the initially proposed single-molecule diffraction methods,[7−17] a 3D structure of a molecule with unknown structure is reconstructed from the average of many single-shot diffraction images of single molecules. In this case, the obtained structure is, strictly speaking, an average structure of the molecule that is constantly fluctuating, and the structural variation of the molecule is averaged out. In contrast, in SOSS, a series of single-molecule diffraction patterns are measured for a molecule, whose static structure is already available, and the distributions of structural parameters of the molecule are sampled from the measured individual diffraction patterns. Therefore, the information on the structure of an object at each instant of fluctuation is kept intact in SOSS.

To verify the concept of SOSS, we performed a computer simulation for a simple diatomic molecule, molecular iodine (I_2). Specifically, we examined the possibility of reconstructing the vibrational wave function of the molecule from a series of single-shot, single-molecule scattering images. The result presented below demonstrates that the vibrational wave function of I_2 can be retrieved using the SOSS method as long as we utilize ultrashort (~1 fs) and intense X-ray pulses. To the best of our knowledge, this paper presents the first work to examine the idea of experimentally probing the entire distribution of structural variation (induced by the fluctuation of a molecule) and ultimately reconstructing vibrational wave functions.

1. Concept. In SOSS, by sampling a significant number of such structural parameters of a fluctuating molecule, we can obtain the distribution of structural variation of the molecule. The obtained distributions of bond length and bond angle are equivalent to the square of the vibrational and rotational wave functions, respectively. In reality, the shape of such a wave function is usually assumed by a model function without experimental verification, but it can be directly probed by SOSS.

To retrieve the structural parameters from each single-object scattering image, we construct a reference library and then adopt a method of correlation mapping into the library. A reference library contains the scattering images calculated for all the possible structures and orientations of the molecule. An example of the reference library for I_2 is shown in Figure 1. For molecular iodine, the diffraction pattern is determined by only one structural parameter, I−I bond length (r), and two orientation parameters (θ and φ) defining the angular orientation with respect to the propagation direction of incoming X-ray beam, as shown in Figure 1a. Therefore, the reference library has the form of three-dimensional matrix, each element of which is a single-molecule scattering image, as shown in Figure 1b.

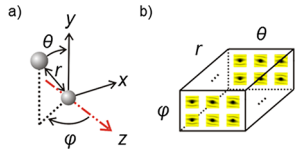

Figure 1. (a) Definition of structural parameters describing an I_2 molecule. We assume that the X-ray pulse propagates along the z axis. (b) A reference library as a function of r, θ, and φ that consists of scattering patterns from single diatomic molecules. An element of this library is a two-dimensional scattering image of a single I_2 molecule whose bond length is r, and angular orientation is designated by θ and φ with respect to the X-ray propagation direction.

By mapping each experimental scattering image into the reference library, we can extract the values for a set of bond length and angular orientation (r, θ, φ). Then, by examining the occurrence distribution of the values of each structural parameter extracted from the scattering images, a probability density function (PDF) of the structural parameter can be reconstructed. In the case of a diatomic molecule, the PDF of bond length (r) between two atoms corresponds to the vibrational PDF, that is, the absolute square of the vibrational wave function. Subsequently, the vibrational wave function can be retrieved from the reconstructed PDF by taking the square root of the PDF and assigning an appropriate sign for each point. We note that, however, the phase information of a wave function cannot be obtained by SOSS. Therefore, the vibrational wave function retrieved by the SOSS experiment corresponds to only the amplitude term of a complete time-dependent wave function. The schematic of reconstructing vibrational wave function from the single-shot, single-molecule scattering images is depicted in Figure 2.

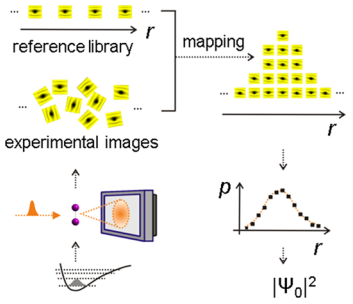

Figure 2. Schematic of retrieving vibrational wave function using SOSS. First, single-shot, single-molecule scattering images of I_2 molecules are collected by scattering experiment. In this work, experimental images were calculated through a simulation instead of being measured. The bond length corresponding to each experimental scattering image is extracted by comparing it with a reference library (i.e., correlation mapping) described in Figure 1. As a result of the mapping, we can obtain an occurrence distribution of the scattering images corresponding to a certain bond length, which represents the PDF of bond length. The obtained PDF can be converted to a vibrational wave function by taking a square root.

2. Simulation. To examine whether the concept of SOSS can be realized experimentally, we performed a series of simulations for molecular iodine. The SOSS simulation is composed of three steps: (1) calculating (instead of measuring) experimental scattering images from molecules of various structures and orientations, of which the distributions are well-defined (for example, by a vibrational wave function), (2) making a reference library from all the possible variations of molecular structure and orientation, and (3) mapping of experimental scattering images into the reference library and reconstructing the PDF of I−I bond length. The details of each step and other considerations are described in the Supporting Information (SI). In particular, we employed a simple ionization model to account for the effect of sample damage (induced by X-ray radiation) on the scattering pattern as described in Section C of the SI.

For an individual set of simulations, a total of 10 000 experimental scattering images were calculated and mapped into the reference library. To calculate a scattering image, we

dx.doi.org/10.1021/jz4016298 | J. Phys. Chem. Lett. 2013, 4, 3345−3350

generated an I_2 molecule of random structure and orientation, of which I−I bond length is governed by a distribution given by a well-defined reference PDF. By mapping each scattering image into the reference library, I−I bond length was extracted from each experimental scattering image. By counting the number of scattering images per each bond length, we reconstructed the occurrence distribution of bond length, that is, PDF of bond length. The agreement between the reconstructed and reference PDFs, which will be defined by two parameters in the next section, varies depending on the experimental condition and thus serves as a measure of the performance of SOSS.

3. Instrument Response. If the SOSS experiment works perfectly, the PDF of bond length reconstructed from the SOSS experiment should exactly match the reference PDF that we start with. However, in reality, the quality of the experimental scattering image is not perfect because of many experimental factors such as the limitation of signal-to-noise ratio, the finite duration of X-ray pulses, and the sample damage by X-ray radiation. Such limitation in the instrument response of the experiment would broaden and shift the PDF reconstructed from the experimental data compared to reference PDF, thus deteriorating the spatial resolution of the experiment. To quantify the broadening of PDF by the instrument response, we need to define a measure of how well the experimental PDF and the reference PDF match each other. Assuming that both PDFs are Gaussian functions, the experimental PDF can be related to reference PDF using a point-spread function (PSF) and a shift function as follows:

$$P^{\mathrm{R}}(r) = (P{*}\mathrm{PSF}{*}S)(r) \tag{1}$$

where $P^{\mathrm{R}}(r)$ is the PDF of bond length reconstructed from the experimental data, $P(r)$ is the reference PDF of bond length, $\mathrm{PSF}(r)$ is the point-spread function, $S(r)$ is the shift function, and * is a convolution operator. In general, the PSF can be assumed to be a Gaussian function centered at $r = 0$:

$$\mathrm{PSF}(r) = a \exp(-r^2/(0.3607 \times \rho^2)) \tag{2}$$

where a is a normalization constant, and ρ is the full width at half-maximum (fwhm) of the Gaussian function. The shift function can be written as a Dirac-delta function:

$$S(r) = \delta(r - \Delta) \tag{3}$$

where Δ is a shift parameter. The width ρ of the PSF and the shift parameter Δ of the shift function can serve as measures of the broadening and shift of PDF, respectively, induced by instrument response. By comparing the reference PDF and the PDF reconstructed from the (simulated) experimental data, we extracted ρ of PSF and Δ of the shift function.

4. Reconstruction of Vibrational Wave Function. We performed the reconstruction of a vibrational wave function while varying the experimental condition including X-ray intensity, pulse duration, angular orientation, and reference PDF. Four different X-ray intensities were used: 10^{10}, 10^{11}, 10^{12}, and 10^{13} photons per spot of 3-nm diameter. The pulse duration of 1 or 3 fs was used because the sample damage is so severe with longer pulses according to a preliminary simulation, which addresses the effect of X-ray radiation on the sample damage as described in Section F of the SI. Three configurations of angular orientation were considered for the I_2 molecule: (1) perfect alignment in one direction, (2) variation of φ with θ fixed at a constant, and (3) variation of θ with φ fixed at a constant. As a reference PDF, three types of functions were used: a delta function, a PDF of I_2 in the ground vibrational state and a PDF of I_2 in the first excited vibrational state, assuming that the I_2 molecule is a harmonic oscillator.

In order to find the experimental condition required to reconstruct a PDF with sufficient spatial resolution (smaller than a few picometers), we first examined the values of ρ and Δ extracted from the reconstructed PDF while changing the experimental parameters of X-ray intensity, pulse duration, and angular orientation. In this case, the delta function was used as the reference PDF. As a result, we found that ρ and Δ become smaller as the X-ray pulse becomes more intense or shorter. Also, it turned out that the quality of reconstructed PDF is not affected by the degree of angular orientation of the I_2 molecule. The detailed procedure and the results of these simulations are described in Section G of the SI.

Then we applied the SOSS method to more realistic reference PDFs than the delta function, that is, the ground-state and the first excited-state vibrational PDFs of I_2. In this case, based on the results of simulations on the delta-function PDF, we employed the X-ray pulse of 1 fs duration and the fixed angular orientation of the I_2 molecule in one direction. The reconstructed PDFs using the ground-state vibrational PDF as the reference PDF are shown in Figure 3. When the X-ray intensity is 10^{10} photons per pulse, the reconstructed PDF is much broader than the reference PDF (Figure 3a). As the X-ray intensity increases, it can be clearly seen that the reconstructed PDF converges to its reference PDF. As the X-ray intensity is increased by a factor of 10, the width of reconstructed PDF becomes much closer to that of reference PDF (Figure 3b). When X-ray intensity is larger than 10^{12} photons per pulse, the reconstructed PDF is nearly indistinguishable from the reference PDF (Figure 3c and 3d). As can be seen in Figure 4, the change in the shape of reconstructed PDF with X-ray intensity is more dramatic when the first excited-state vibrational PDF is used as the reference PDF. With the X-ray intensity of 10^{10} photons/pulse, the

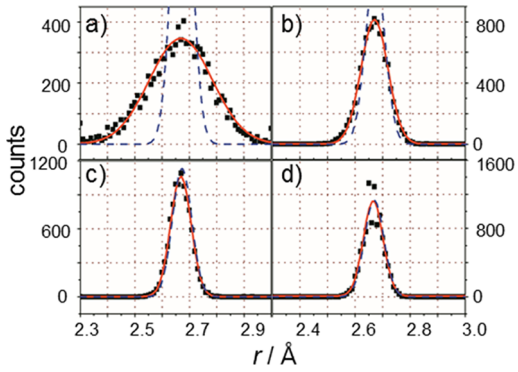

Figure 3. Reconstructed PDFs of bond length using the vibrational PDF of the ground-state harmonic oscillator as reference PDF. Various X-ray intensities were used: (a) 10^{10}, (b) 10^{11}, (c) 10^{12}, and (d) 10^{13} photons per pulse. A total of 10 000 experimental scattering images were calculated with a reference PDF (blue dashed line), which is the square of the vibrational wave function of a harmonic oscillator in the ground state. We assumed that the I_2 molecule is perfectly aligned in one direction, and the temporal duration of an X-ray pulse was set to be 1 fs. Black squares represent the occurrence of scattering images corresponding to a certain bond length. Red solid lines are the fits of the black squares using eq 1 and represent the reconstructed PDF of bond length. Note that *y*-scales are different between the plots.

dx.doi.org/10.1021/jz4016298 | J. Phys. Chem. Lett. 2013, 4, 3345−3350

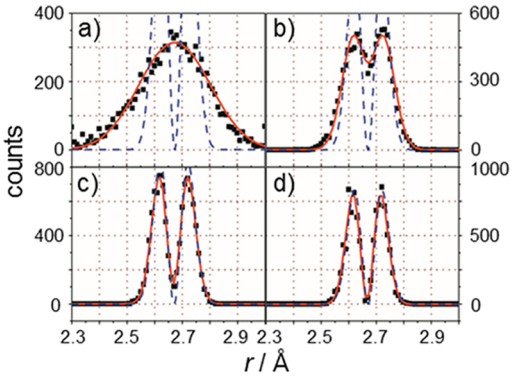

Figure 4. Reconstructed PDFs of bond length using the vibrational PDF of a harmonic oscillator in the first excited state as reference PDF. Other conditions are the same as in Figure 3 except that the reference PDF (blue dashed line) is the square of the vibrational wave function of a harmonic oscillator in the first excited state. Note that *y*-scales are different between the plots.

reconstructed PDF for the first excited-state vibrational PDF (Figure 4a) has a Gaussian shape and significantly deviates from the reference PDF. However, as the X-ray intensity increases, a broad peak of reconstructed PDF becomes split into two peaks (Figure 4b–d). With X-ray intensity larger than 10^{12} photons per pulse, the two peaks are clearly resolved as shown in Figure 4c,d with a zero-intensity vibrational node between the two peaks being observed.

To quantitatively assess the reconstruction of a vibrational wave function, the reconstructed PDFs were fitted using eqs 1, 2, and 3 to estimate the parameters, ρ and Δ, of the instrument response. The resulting values of ρ and Δ are shown in Table 1.

Table 1. Result of PDF Reconstruction Using SOSS under Various Experimental Conditions

reference PDF	pulse intensity (photons/pulse)	peak shift, Δ (Å)	broadening, ρ (Å, fwhm)
ground[a]	10^{10}	−0.001	0.260
ground[a]	10^{11}	0	0.080
ground[a]	10^{12}	−0.002	0.030
ground[a]	10^{13}	−0.005	0.013
first excited[b]	10^{10}	0.003	0.261
first excited[b]	10^{11}	0	0.077
first excited[b]	10^{12}	−0.002	0.029
first excited[b]	10^{13}	−0.005	0.015

The parameters defining the broadening (ρ) and shift (Δ) of PDF induced by instrument response was calculated by fitting of the reconstructed PDF based on eqs 1, 2, and 3. [a]Vibrational PDF of a harmonic oscillator in the ground state. [b]Vibrational PDF of a harmonic oscillator in the first excited state.

We can see that the values of ρ and Δ for the two different reference PDFs (that is, ground-state and excited-state vibrational PDFs) are almost the same. For a small photon flux, 10^{10} photons per pulse, the reconstructed PDF exhibits a ρ value of 0.26 Å, which is not sufficient to depict the molecular vibration occurring on the length scale of picometers. The poor spatial resolution is attributed to the lack of the number of photons scattered to the detector. When the X-ray intensity is 10^{12} photons per pulse, ρ is ∼0.03 Å, which should be good enough to reproduce the detailed features of the ground-state and the first excited-state vibrational wave functions of I_2. Unlike ρ, the shift parameter Δ, which reflects the shift introduced by instrument response, is not affected by the X-ray intensity and stays nearly zero.

In this work, we demonstrated the prospect of retrieving the vibrational wave function of I_2 using SOSS as long as we can capture instantaneous structures of a fluctuating molecule using femtosecond X-ray pulses. We suggest that the PDF of bond lengths can be reconstructed using the SOSS method as long as the X-ray pulse of sufficiently short duration (1 fs) and high intensity (10^{12} photons per pulse) is used. Subsequently, the reconstructed vibrational PDF can be converted to the amplitude term of the vibrational wave function.

For the realization of the SOSS experiment, there still remain several technical obstacles to overcome. Unless photon flux and/or focusing size of an X-ray pulse is further improved than currently available, a typical single-shot, single-object scattering image would not contain high enough intensity for the structural analysis. To minimize the error accompanying the reconstruction of the PDF, we estimate that high intensity (>10^{12} photons per pulse) and ultratight focusing (3 nm ×3 nm focusing size) of the X-ray pulse is required. The intensity of 10^{12} photons per pulse is already available at XFEL. The focusing size of 3 nm ×3 nm is still far from currently available focusing range (∼1 μm at XFEL, and ∼7 nm at third-generation synchrotron source).[18−21] However, considering that the X-ray focusing technique is developing rapidly, we expect that the desired focal size can be achieved in the near future. As an alternative, if we utilize more intense X-ray than 10^{12} photons per pulse, which should be available in the future versions of XFELs, a little looser focusing might be acceptable in terms of photon density. While the increase of the X-ray fluence is required, it is also important to consider an appropriate method of providing fresh sample for the measurement because an intense X-ray pulse will completely destroy the target molecule even after a single interaction with the molecule. For that purpose, a molecular beam generated by supersonic expansion can be a good solution to supply fresh sample for each X-ray pulse because of its well-defined kinetic energy and dramatic cooling of molecules.[22,23] In addition, it would be very difficult to efficiently supply the molecular beam into the extremely small X-ray focal spot (3 nm ×3 nm) required for the SOSS experiment. As a result, it is expected that many scattering patterns with nearly zero intensities will be measured from the molecules not perfectly located within the X-ray focal spot. We believe that such scattering patterns from the misaligned molecules can be easily sorted out from the data due to their small intensities.

The biggest advantage of SOSS is the sensitivity to rarely populated structures that have short lifetimes and low populations. According to the result of our simulation, it is possible to capture the structure of the rarely populated states using the SOSS method. For example, in Figure 4, we can see that the molecules with r = 2.52 Å and r = 2.80 Å are counted in the PDF of bond length despite their extremely low occurrences. Such rarely populated states are often obscured in ensemble measurements, where the measured signal is dominated by only highly populated configurations. In this sense, the SOSS method may serve as an excellent tool for structural characterization of rarely populated states. In chemical reactions[24−27] and biological processes,[28−31] the states with extremely low population can play important roles

dx.doi.org/10.1021/jz4016298 | J. Phys. Chem. Lett. 2013, 4, 3345−3350

in the dynamic processes. For a complete understanding of those processes, it is crucial to characterize the structure of those rarely populated states. As an example, when implemented in combination with time-resolved techniques,[32−36] SOSS can be utilized to capture the transition states of a chemical reaction that lie along the reaction coordinate. Additionally, we discuss further applications of SOSS in Section H of the SI.

■ ASSOCIATED CONTENT

Supporting Information

Description of assumptions; X-ray pulse characteristics; ionization model; details of the scattering pattern calculation; details of making reference library and mapping; the effect of X-ray pulse parameters on the sample damage, and the effect of experimental conditions on the instrument response function; further applications of SOSS; comparison with ultrafast vibrational spectroscopy. This material is available free of charge via the Internet at http://pubs.acs.org.

■ AUTHOR INFORMATION

Corresponding Author

*E-mail: hyotcherl.ihee@kaist.ac.kr.

Author Contributions

⊥These authors contributed equally to this work.

Notes

The authors declare no competing financial interest.

■ ACKNOWLEDGMENTS

This work was supported by Institute for Basic Science (IBS). This work was supported by an Inha University Research Grant (INHA-48581).

■ REFERENCES

(1) Fitter, J.; Katranidis, A.; Rosenkranz, T.; Atta, D.; Schlesinger, R.; Buldt, G. Single Molecule Fluorescence Spectroscopy: A Tool for Protein Studies Approaching Cellular Environmental Conditions. *Soft Matter* **2011**, *7*, 1254−1259.

(2) Haran, G. Single-Molecule Raman Spectroscopy: A Probe of Surface Dynamics and Plasmonic Fields. *Acc. Chem. Res.* **2010**, *43*, 1135−1143.

(3) Celebrano, M.; Kukura, P.; Renn, A.; Sandoghdar, V. Single-Molecule Imaging by Optical Absorption. *Nat. Photonics* **2011**, *5*, 95−98.

(4) Roiter, Y.; Minko, S. AFM Single Molecule Experiments at the Solid-Liquid Interface: In Situ Conformation of Adsorbed Flexible Polyelectrolyte Chains. *J. Am. Chem. Soc.* **2005**, *127*, 15688−15689.

(5) Neuman, K. C.; Nagy, A. Single-Molecule Force Spectroscopy: Optical Tweezers, Magnetic Tweezers and Atomic Force Microscopy. *Nat. Methods* **2008**, *5*, 491−505.

(6) Ihee, H. Novel Single-Molecule Technique by Single-Object Scattering Sampling (SOSS). *Bull. Korean Chem. Soc.* **2011**, *32*, 1849−1850.

(7) Spence, J. C. H.; Doak, R. B. Single Molecule Diffraction. *Phys. Rev. Lett.* **2004**, *92*, 198102.

(8) Miao, J. W.; Charalambous, P.; Kirz, J.; Sayre, D. Extending the Methodology of X-Ray Crystallography to Allow Imaging of Micrometre-Sized Non-Crystalline Specimens. *Nature* **1999**, *400*, 342−344.

(9) Neutze, R.; Wouts, R.; van der Spoel, D.; Weckert, E.; Hajdu, J. Potential for Biomolecular Imaging with Femtosecond X-ray Pulses. *Nature* **2000**, *406*, 752−757.

(10) Hajdu, J. Single-Molecule X-ray Diffraction. *Curr. Opin. Struct. Biol.* **2000**, *10*, 569−573.

(11) Miao, J.; Hodgson, K. O.; Sayre, D. An Approach to Three-Dimensional Structures of Biomolecules by Using Single-Molecule Diffraction Images. *Proc. Natl. Acad. Sci. U.S.A.* **2001**, *98*, 6641−6645.

(12) Webster, G.; Hilgenfeld, R. Perspectives on Single Molecule Diffraction Using the X-ray Free Electron Laser. *Single Mol.* **2002**, *3*, 63−68.

(13) Seibert, M. M.; Ekeberg, T.; Maia, F. R.; Svenda, M.; Andreasson, J.; Jonsson, O.; Odic, D.; Iwan, B.; Rocker, A.; Westphal, D.; et al. Single Mimivirus Particles Intercepted and Imaged with an X-ray Laser. *Nature* **2011**, *470*, 78−81.

(14) Yoon, C. H.; Schwander, P.; Abergel, C.; Andersson, I.; Andreasson, J.; Aquila, A.; Bajt, S.; Barthelmess, M.; Barty, A.; Bogan, M. J.; et al. Unsupervised Classification of Single-Particle X-ray Diffraction Snapshots by Spectral Clustering. *Opt. Express* **2011**, *19*, 16542−16549.

(15) Bogan, M. J.; Benner, W. H.; Boutet, S.; Rohner, U.; Frank, M.; Barty, A.; Seibert, M. M.; Maia, F.; Marchesini, S.; Bajt, S.; et al. Single Particle X-ray Diffractive Imaging. *Nano Lett.* **2008**, *8*, 310−316.

(16) Bogan, M. J.; Boutet, S.; Barty, A.; Benner, W. H.; Frank, M.; Lomb, L.; Shoeman, R.; Starodub, D.; Seibert, M. M.; Hau-Riege, S. P.; et al. Single-Shot Femtosecond X-ray Diffraction from Randomly Oriented Ellipsoidal Nanoparticles. *Phys. Rev. Spec. Top.—Accel. Beams* **2010**, *13*, 094701.

(17) Loh, N. D.; Bogan, M. J.; Elser, V.; Barty, A.; Boutet, S.; Bajt, S.; Hajdu, J.; Ekeberg, T.; Maia, F. R. N. C.; Schulz, J.; et al. Cryptotomography: Reconstructing 3D Fourier Intensities from Randomly Oriented Single-Shot Diffraction Patterns. *Phys. Rev. Lett.* **2010**, *104*, 225501.

(18) Yumoto, H.; Mimura, H.; Koyama, T.; Matsuyama, S.; Tono, K.; Togashi, T.; Inubushi, Y.; Sato, T.; Tanaka, T.; Kimura, T.; et al. Focusing of X-Ray Free-Electron Laser Pulses with Reflective Optics. *Nat. Photonics* **2013**, *7*, 43−47.

(19) Mimura, H.; Handa, S.; Kimura, T.; Yumoto, H.; Yamakawa, D.; Yokoyama, H.; Matsuyama, S.; Inagaki, K.; Yamamura, K.; Sano, Y.; et al. Breaking the 10 nm Barrier in Hard-X-ray Focusing. *Nat. Phys.* **2010**, *6*, 122−125.

(20) Takano, H.; Tsuji, T.; Hashimoto, T.; Koyama, T.; Tsusaka, Y.; Kagoshima, Y. Sub-15nm Hard X-ray Focusing with a New Total-Reflection Zone Plate. *Appl. Phys. Express* **2010**, *3*, 076702.

(21) Yamauchi, K.; Mimura, H.; Kimura, T.; Yumoto, H.; Handa, S.; Matsuyama, S.; Arima, K.; Sano, Y.; Yamamura, K.; Inagaki, K.; et al. Single-Nanometer Focusing of Hard X-rays by Kirkpatrick−Baez Mirrors. *J. Phys.: Condens. Matter* **2011**, *23*, 394206.

(22) Van De Meerakker, S. Y. T.; Bethlem, H. L.; Meijer, G. Taming Molecular Beams. *Nat. Phys.* **2008**, *4*, 595−602.

(23) Levy, D. H. The Spectroscopy of Very Cold Gases. *Science* **1981**, *214*, 263−269.

(24) Lee, J. H.; Wulff, M.; Bratos, S.; Petersen, J.; Guerin, L.; Leicknam, J. C.; Carnmarata, M.; Kong, Q.; Kim, J.; Moller, K. B.; et al. Filming the Birth of Molecules and Accompanying Solvent Rearrangement. *J. Am. Chem. Soc.* **2013**, *135*, 3255−3261.

(25) Kim, J.; Lee, J. H.; Kim, J.; Jun, S.; King, K. H.; Kim, T. W.; Wulff, M.; Ihee, H. Structural Dynamics of 1,2-Diiodoethane in Cyclohexane Probed by Picosecond X-ray Liquidography. *J. Phys. Chem. A* **2012**, *116*, 2713−2722.

(26) Kong, Q.; Lee, J. H.; Kim, K. H.; Kim, J.; Wulff, M.; Ihee, H.; Koch, M. H. J. Ultrafast X-ray Solution Scattering Reveals Different Reaction Pathways in the Photolysis of Triruthenium Dodecacarbonyl ($Ru_3(CO)_{12}$) after Ultraviolet and Visible Excitation. *J. Am. Chem. Soc.* **2010**, *132*, 2600−2607.

(27) Kim, T. K.; Lorenc, M.; Lee, J. H.; Russo, M.; Kim, J.; Cammarata, M.; Kong, Q. Y.; Noel, S.; Plech, A.; Wulff, M.; et al. Spatiotemporal Reaction Kinetics of an Ultrafast Photoreaction Pathway Visualized by Time-Resolved Liquid X-ray Diffraction. *Proc. Natl. Acad. Sci. U.S.A.* **2006**, *103*, 9410−9415.

(28) Kim, T. W.; Lee, J. H.; Choi, J.; Kim, K. H.; van Wilderen, L. J.; Guerin, L.; Kim, Y.; Jung, Y. O.; Yang, C.; Kim, J.; et al. Protein Structural Dynamics of Photoactive Yellow Protein in Solution

Revealed by Pump−Probe X-ray Solution Scattering. *J. Am. Chem. Soc.* **2012**, *134*, 3145−3153.
(29) Tomita, A.; Sato, T.; Ichiyanagi, K.; Nozawa, S.; Ichikawa, H.; Chollet, M.; Kawai, F.; Park, S. Y.; Tsuduki, T.; Yamato, T.; et al. Visualizing Breathing Motion of Internal Cavities in Concert with Ligand Migration in Myoglobin. *Proc. Natl. Acad. Sci. U.S.A.* **2009**, *106*, 2612−2616.
(30) Witkoskie, J. B.; Cao, J. S. Analysis of the Entire Sequence of a Single Photon Experiment on a Flavin Protein. *J. Phys. Chem. B* **2008**, *112*, 5988−5996.
(31) Kim, K. H.; Muniyappan, S.; Oang, K. Y.; Kim, J. G.; Nozawa, S.; Sato, T.; Koshihara, S. Y.; Henning, R.; Kosheleva, I.; Ki, H.; et al. Direct Observation of Cooperative Protein Structural Dynamics of Homodimeric Hemoglobin from 100 ps to 10 ms with Pump−Probe X-ray Solution Scattering. *J. Am. Chem. Soc.* **2012**, *134*, 7001−7008.
(32) Neutze, R.; Moffat, K. Time-Resolved Structural Studies at Synchrotrons and X-ray Free Electron Lasers: Opportunities and Challenges. *Curr. Opin. Struct. Biol.* **2012**, *22*, 651−659.
(33) Aquila, A.; Hunter, M. S.; Doak, R. B.; Kirian, R. A.; Fromme, P.; White, T. A.; Andreasson, J.; Arnlund, D.; Bajt, S.; Barends, T. R. M.; et al. Time-Resolved Protein Nanocrystallography Using an X-ray Free-Electron Laser. *Opt. Express* **2012**, *20*, 2706−2716.
(34) Barty, A. Time-Resolved Imaging Using X-ray Free Electron Lasers. *J. Phys. B: At., Mol. Opt. Phys.* **2010**, *43*, 194014.
(35) Glownia, J. M.; Cryan, J.; Andreasson, J.; Belkacem, A.; Berrah, N.; Blaga, C. I.; Bostedt, C.; Bozek, J.; DiMauro, L. F.; Fang, L.; et al. Time-Resolved Pump-Probe Experiments at the LCLS. *Opt. Express* **2010**, *18*, 17620−17630.
(36) Spence, J. C. H.; Weierstall, U.; Chapman, H. N. X-ray Lasers for Structural and Dynamic Biology. *Rep. Prog. Phys.* **2012**, *75*, 102601.